




# Hydrothermal syntheses, crystal structures, and luminescent properties of two Mn(II) coordination polymers based on carboxylate and imidazole-containing ligands

Jingxia Wang & Ning Sheng

To cite this article: Jingxia Wang & Ning Sheng (2015) Hydrothermal syntheses, crystal structures, and luminescent properties of two Mn(II) coordination polymers based on carboxylate and imidazole-containing ligands, *Journal of Coordination Chemistry*, 68:7, 1273-1281, DOI: [10.1080/00958972.2015.1018194](https://doi.org/10.1080/00958972.2015.1018194)


To link to this article: <http://dx.doi.org/10.1080/00958972.2015.1018194>

 View supplementary material 

 Accepted author version posted online: 16 Feb 2015.  
Published online: 13 Mar 2015.

 Submit your article to this journal 

 Article views: 49

 View related articles 

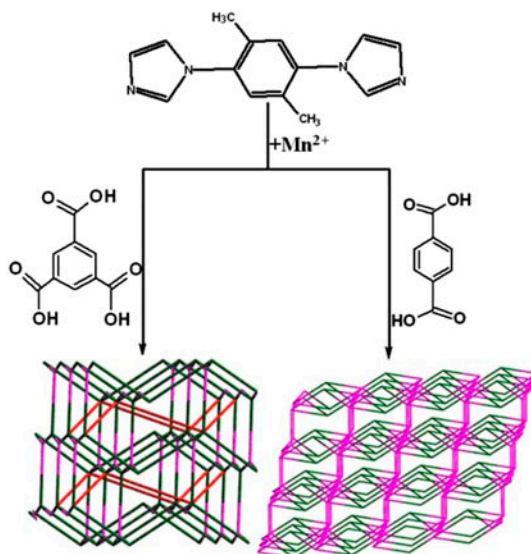
 View Crossmark data 

## Hydrothermal syntheses, crystal structures, and luminescent properties of two Mn(II) coordination polymers based on carboxylate and imidazole-containing ligands

JINGXIA WANG\* and NING SHENG

Department of Chemistry and Chemical Engineering, Key Laboratory of Inorganic Chemistry in Universities of Shandong, Jining University, Qufu, PR China

(Received 27 March 2014; accepted 26 January 2015)



Two new coordination polymers,  $[\text{Mn}(1,4\text{-BDC})(\text{bimb})_{0.5}]_n$  (**1**) and  $[\text{Mn}(\text{H}_3\text{btc})(\text{bimb})_{0.5}]_n$  (**2**) (1,4-H<sub>2</sub>BDC = 1,4-benzenedicarboxylic acid, H<sub>3</sub>btc = 1,3,5-benzenetricarboxylic acid and bimb = 1,4-bis(1-imidazol-yl)-2,5-dimethyl benzene), have been hydrothermally synthesized by reactions of Mn(II) salt with a rigid 1,4-bis(1-imidazol-yl)-2,5-dimethyl benzene and varying carboxylate ligands. Complex **1** is a binodal (3,7)-connected 3-D architecture with point symbol  $(4^9.6^{17}).(6^3)$ . Complex **2** is a (3,6)-connected 3-D structure with point symbol  $(3.4.5).(3^2.4^2.5.6^3.7^2)$ . The luminescent properties of **1** and **2** were investigated in the solid state at room temperature.

**Keywords:** Mn(II); Crystal structure; Luminescent property

\*Corresponding author. Email: [jnwangjx@163.com](mailto:jnwangjx@163.com)

## 1. Introduction

The construction of new coordination polymers (CPs) has received interest for intriguing structures and topological nets and for applications as functional materials in magnetism, gas adsorption, catalysis, luminescence, etc. [1–16]. To construct new CPs, efforts have been devoted to modification of the ligands to control the structures of CPs because the geometries of ligands have a great effect on the structural frameworks of CPs [17–19]. For self-assembly processes of CPs, the mixed-ligand strategy of multicarboxylate and N-donor ligands is an effective method for construction of the new frameworks with greater tunability of structural frameworks than single ligands [20, 21]. Among N-donor bridging ligands, imidazole-containing ligands have been employed to construct CPs due to their flexible and diverse coordination modes which can lead to topologies such as cages, honeycombs, polycatenation, and interpenetration. [22–24]. CPs constructed from rigid bidentate 1,4-bis(1-imidazol-yl)-2,5-dimethyl benzene are seldom reported [25–31]. In bimb, the two imidazole rings can rotate around the central phenyl ring with a variety of intriguing structures obtained. Introduction of different carboxylates as anions have been adopted in CPs because of their diverse coordination modes [32, 33].

We employed the mixed-ligand strategy of the rigid imidazole-containing ligand (bimb) and different carboxylate ligands, synthesizing two Mn(II) CPs,  $[\text{Mn}(1,4\text{-BDC})(\text{bimb})_{0.5}]_n$  (**1**) and  $[\text{Mn}(\text{Hbtc})(\text{bimb})_{0.5}]_n$  (**2**). Complexes **1** and **2** feature different frameworks which indicate that organic carboxylate ligands impact the CPs structure. Luminescent properties of **1** and **2** were investigated.

## 2. Experimental

### 2.1. Materials and physical measurements

All reagents and solvents were commercially available and used as received. Elemental analysis was carried out on a Carlo Erba 1106 full-automatic trace organic elemental analyzer. FT-IR spectra were recorded with a Bruker Equinox 55 FT-IR spectrometer as a dry KBr pellet from 400 to 4000  $\text{cm}^{-1}$ . Solid-state fluorescence spectra were recorded on a Hitachi F-4600 equipped with a xenon lamp and a quartz carrier at room temperature. TG analyses were carried out with a Mettler Toledo TGA 851e analyzer with a heating rate of 10  $^{\circ}\text{C min}^{-1}$  under nitrogen.

### 2.2. Synthesis

**2.2.1. Preparation of  $[\text{Mn}(1,4\text{-BDC})(\text{bimb})_{0.5}]_n$  (**1**).** A mixture of  $\text{MnCl}_2 \cdot 4\text{H}_2\text{O}$  (0.099 g, 0.5 mM), 1,4- $\text{H}_2\text{BDC}$  (0.083 g, 0.5 mM), bimb (0.105 g, 0.5 mM), NaOH (0.04 g, 1 mM), and deionized water (15 mL) were heated at 140  $^{\circ}\text{C}$  for 72 h and then cooled to room temperature at 5  $^{\circ}\text{C h}^{-1}$ . Brown block crystals were obtained and washed with alcohol several times and then dried at the room temperature (Yield: 72% and 0.121 g based on Mn). Elemental Anal. Calcd (%) for  $\text{C}_{15}\text{H}_{11}\text{MnN}_2\text{O}_4$ : C, 53.27; H, 3.28; N, 8.28. Found: C, 53.30; H, 3.29; N, 8.26. IR ( $\text{cm}^{-1}$ , KBr pellet): 3046 (w, C–H), 2088 (w, C–H), 1630 (s,  $\text{COO}^-$ ), 1522 (s,  $\text{COO}^-$ ), 1407 (s,  $\text{COO}^-$ ), 1355 (s,  $\text{COO}^-$ ), 1259 (m, C–H), 1051 (s, C–H), 931 (m, C–H), 807 (m, C–H), 722 (w, N–M), 679 (m, O–M).

**2.2.2. Preparation of [Mn(Hbtc)(bimb)<sub>0.5</sub>]<sub>n</sub> (2).** The same synthetic procedure as that for **1** was used, except that H<sub>3</sub>btc (0.114 g, 0.5 mM) was used in place of 1,4-H<sub>2</sub>BDC. Yellow block crystals were obtained and washed with alcohol several times and then dried at room temperature (Yield: 73% and 0.140 g based on Mn). Elemental Anal. Calcd (%) for C<sub>16</sub>H<sub>11</sub>MnN<sub>2</sub>O<sub>4</sub>: C, 50.28; H, 2.90; N, 7.33. Found: C, 50.32; H, 2.91; N, 7.30. IR (cm<sup>-1</sup>, KBr pellet): 3098 (w, C–H), 2964 (w, C–H), 1682 (s, –COOH), 1627 (s, COO<sup>-</sup>), 1508 (m, COO<sup>-</sup>), 1480 (s, COO<sup>-</sup>), 1379 (w, COO<sup>-</sup>), 1217 (m, C–H), 1150 (m, C–H), 1044 (s, C–H), 967 (s, C–H), 858 (m, C–H), 741 (m, N–M), 603 (w, O–M).

### 2.3. X-ray data collection and structure determinations

Single crystals of **1** and **2** were prepared. X-ray crystallographic data of **1** and **2** were collected at room temperature using epoxy-coated crystals mounted on a glass fiber. All measurements were made on a Bruker SMART APEXII CCD diffractometer equipped with graphite monochromated Mo-*K*α radiation ( $\lambda = 0.71073$  Å) using a  $\omega$ -scan mode. Empirical absorption correction was applied using SADABS [34]. All the structures were solved by direct methods and refined by full-matrix least squares on  $F^2$  using SHELX 97 [35]. All non-hydrogen atoms were refined anisotropically. Hydrogens were located by geometric calculations, and their positions and thermal parameters were fixed during the structure refinement. The crystallographic data and experimental details of structural analyses for CPs are summarized in table 1. Selected bond and angle parameters are listed in table 2.

Table 1. Crystallographic data and details of diffraction experiments for **1** and **2**.

	<b>1</b>	<b>2</b>
Formula	C <sub>15</sub> H <sub>11</sub> MnN <sub>2</sub> O <sub>4</sub>	C <sub>16</sub> H <sub>11</sub> MnN <sub>2</sub> O <sub>6</sub>
$M_r$	338.20	382.21
$T$ (K)	293(2)	293(2)
$\lambda$ (Å)	0.71073	0.71073
Crystal system	Monoclinic	Triclinic
Space group	$P2_1/c$	$P-1$
$a$ (Å)	8.860(9)	8.6710(10)
$b$ (Å)	16.640(5)	8.7130(10)
$c$ (Å)	20.252(11)	10.3780(10)
$\alpha$ (°)	90.000	104.8270(10)
$\beta$ (°)	105.890(16)	95.6820(10)
$\gamma$ (°)	90.000	103.5030(10)
$V$ (Å <sup>3</sup> )	2872(2)	726.42(14)
$Z$	4	2
$F(000)$	1376	388
$\mu$ (mm <sup>-1</sup> )	0.938	0.949
$\rho$ (g cm <sup>-3</sup> )	1.565	1.747
$R_{int}$	0.0240	0.013
$R^a$ , $wR^b$ [ $I > 2\sigma(I)$ ]	$R_1 = 0.0307$ $wR_2 = 0.0769$	$R_1 = 0.0252$ $wR_2 = 0.0659$
$R^a$ , $wR^b$ (all data)	$R_1 = 0.0424$ , $wR_2 = 0.0833$	$R_1 = 0.0252$ $wR_2 = 0.0661$
Gof	1.035	1.096
Max/min (e Å <sup>-3</sup> )	0.419/–0.361	0.237/–0.297

$$^a R = \frac{\sum(|F_o| - |F_c|)}{\sum|F_o|}$$

$$^b wR = \left[ \frac{\sum w(|F_o|^2 - |F_c|^2)^2}{\sum w(F_o^2)} \right]^{1/2}$$

Table 2. Selected bond lengths (Å) and angles (°) for **1** and **2**.

<b>1</b>			
Mn1–O4	2.1554(14)	Mn1–N1	2.2361(16)
Mn1–O2	2.1601(16)	Mn2–O1	2.0492(14)
Mn1–O7 <sup>i</sup>	2.1820(15)	Mn2–O3	2.0627(14)
Mn1–N3	2.2156(16)	Mn2–O6 <sup>ii</sup>	2.0690(16)
Mn1–O8	2.2352(13)	Mn2–O5	2.2019(15)
Mn2–O8	2.2854(17)		
O4–Mn1–O2	91.01(6)	O7 <sup>i</sup> –Mn1–N1	99.17(6)
O4–Mn1–O7 <sup>i</sup>	86.71(5)	N3–Mn1–N1	89.69(6)
O2–Mn1–O7 <sup>i</sup>	168.28(5)	O8–Mn1–N1	171.07(5)
O4–Mn1–N3	176.21(6)	O1–Mn2–O3	121.23(6)
O2–Mn1–N3	88.49(6)	O1–Mn2–O6 <sup>ii</sup>	96.19(6)
O7 <sup>i</sup> –Mn1–N3	94.53(6)	O3–Mn2–O6 <sup>ii</sup>	96.23(6)
O4–Mn1–O8	85.22(5)	O1–Mn2–O5	115.35(6)
O2–Mn1–O8	84.50(6)	O3–Mn2–O5	120.72(7)
O7 <sup>i</sup> –Mn1–O8	83.85(6)	O6 <sup>ii</sup> –Mn2–O5	93.96(5)
N3–Mn1–O8	98.47(6)	O1–Mn2–O8	104.19(6)
O4–Mn1–N1	86.57(6)	O3–Mn2–O8	91.33(6)
O2–Mn1–N1	92.16(6)	O6 <sup>ii</sup> –Mn2–O8	150.43(5)
O5–Mn2–O8	58.04(5)		
<b>2</b>			
Mn1–O1	2.1243(12)	Mn1–N1	2.2199(15)
Mn1–O5 <sup>i</sup>	2.1241(13)	Mn1–O6 <sup>iii</sup>	2.2754(12)
Mn1–O2 <sup>ii</sup>	2.1449(13)	Mn1–O4	2.3428(13)
O5 <sup>i</sup> –Mn1–O1	87.07(5)	O1–Mn1–O6 <sup>iii</sup>	86.35(5)
O5 <sup>i</sup> –Mn1–O2 <sup>ii</sup>	99.68(5)	O2 <sup>ii</sup> –Mn1–O6 <sup>iii</sup>	157.87(5)
O1–Mn1–O2 <sup>ii</sup>	97.04(5)	N1–Mn1–O6 <sup>iii</sup>	89.35(5)
O5 <sup>i</sup> –Mn1–N1	96.31(6)	O5 <sup>i</sup> –Mn1–O4	172.70(5)
O1–Mn1–N1	175.02(5)	O1–Mn1–O4	85.73(5)
O2 <sup>ii</sup> –Mn1–N1	86.02(5)	O2 <sup>ii</sup> –Mn1–O4	82.43(5)
O5 <sup>i</sup> –Mn1–O6 <sup>iii</sup>	102.34(5)	N1–Mn1–O4	90.79(5)

Symmetry codes: For **1** (i)  $x-1, -y+3/2, z-1/2$ ; (ii)  $x, -y+3/2, z-1/2$ ; For **2**: (i)  $x-1, y, z$ ; (ii)  $-x+1, -y, -z+1$ ; (iii)  $-x+2, -y+1, -z+1$ .

### 3. Results and discussion

#### 3.1. Description of crystal structures

**3.1.1. [Mn(1,4-BDC)(bimb)<sub>0.5</sub>]<sub>n</sub> (1).** Single-crystal X-ray analysis reveals that the asymmetric unit of **1** consists of two Mn(II) centers, two 1,4-BDC, and one bimb with triclinic system space group  $P-1$ . As shown in figure 1(a), the Mn1 has a distorted octahedral geometry, ligated by three carboxylate oxygens, and one nitrogen in the equatorial plane, and O4 from carboxylate and N3 from bimb at the apical positions with the O4–Mn1–N3 angle of 176.21(6)°. The Mn2 center is five-coordinate with five carboxylate oxygens with a distorted square-pyramidal geometry. In **1**, the carboxylates are  $\mu_2: \eta^1/\eta^2$  (chelating/bridging) and  $\mu_2: \eta^1/\eta^1$  [bis(bridging-bidentate)] coordination. In **1**, the carboxylate groups containing O1, O2, O3, O4, O6, and O7 adopt  $\mu_2: \eta^1/\eta^1$  coordination in which the Mn–O distances are 2.0492(14) Å, 2.1601(16) Å, 2.0627(14) Å, 2.1554(14) Å, 2.0690(16) Å, and 2.1820(15) Å, respectively. The carboxylates containing O5 and O8 are  $\mu_2: \eta^1/\eta^2$  in which the Mn–O distances are 2.2019(15) Å, 2.2854(17) Å, and 2.2019(15) Å. The Mn–N bond lengths are 2.236(16) Å and 2.216(16) Å. Two independent Mn(II) centers are bridged by three carboxylates (O1–C1–O2:  $\mu_2: \eta^1/\eta^1$ , O3–C8–O4:  $\mu_2: \eta^1/\eta^1$ , and O5–C23–O8:  $\mu_2: \eta^1/\eta^2$ ) to form a dinuclear unit with Mn–Mn distance of 3.586 Å. In **1**, Mn(II) cations are bridged by carboxylates to form a rod-like chain. These chains as infinite rod-shaped secondary building

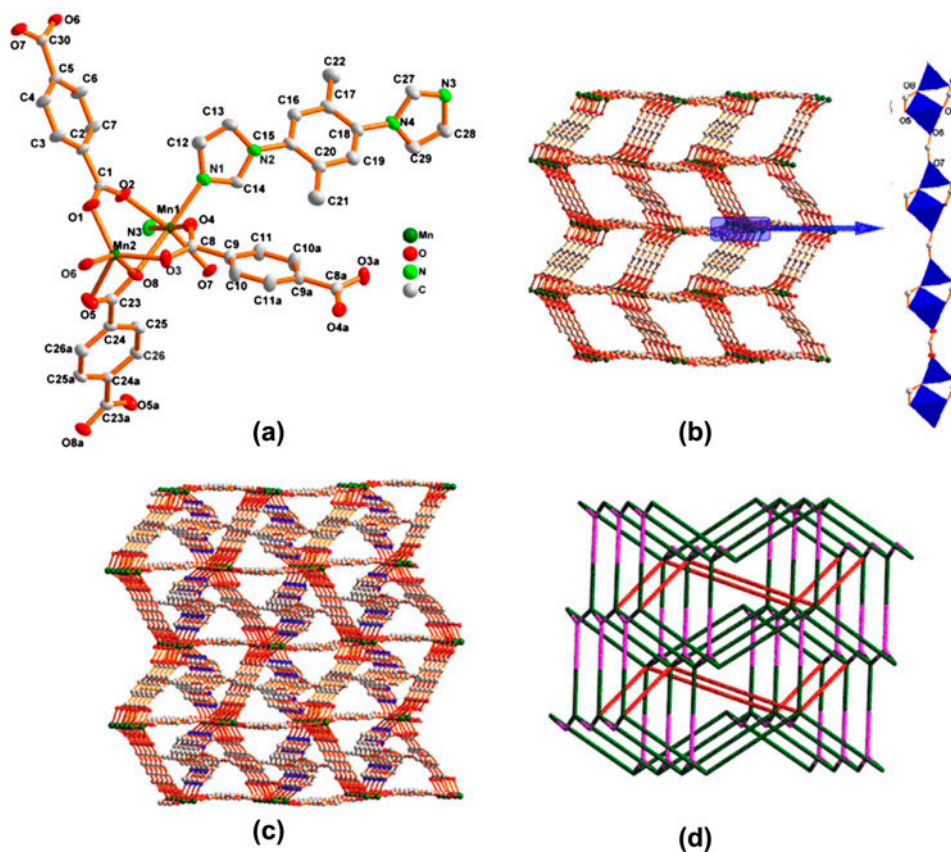


Figure 1. (a) The coordination environment of Mn(II) in **1** with 50% thermal ellipsoids drawn at 50% probability. Hydrogens are omitted for clarity; (b) Left: the 3-D Mn(II)-carboxylate framework; right: the chain formed from the SBUs with two corner-sharing Mn polyhedral; (c) The final 3-D framework constructed by Mn-carboxylate-bimb system; (d) The (3,7)-connected topology for **1**. The red lines: bimb ligands. The other color lines: carboxylate ligands (see <http://dx.doi.org/10.1080/00958972.2015.1018194> for color version).

units are further interlinked by carboxylate ligands to produce a 3-D network with a large window (approximate  $11.440 \times 18.946 \text{ \AA}$  based on the Mn1...Mn1 distance) [figure 1(b)]. The bimb ligands lie in the large windows and connect Mn ions [figure 1(c)]. From the viewpoint of topology by topos software [36–38], this final 3-D structure can be represented as a (3,7)-connected net with  $(4^4.6^{17}).(6^3)$  by reducing the dinuclear Mn unit and BDC<sup>2-</sup> ligand as the 7-connected and 3-connected nodes, respectively [figure 1(d)]. In **1**, the total void value is estimated to be  $114 \text{ \AA}^3$ , approximately  $4.0\% \text{ \AA}^3$  of the total crystal volume of  $2872.0 \text{ \AA}^3$  by Platon.

**3.1.2. [Mn(Hbtc)(bimb)<sub>0.5</sub>]<sub>n</sub> (2).** Single-crystal X-ray diffraction analysis reveals the asymmetric unit consists of one crystallographically independent Mn(II), one Hbtc<sup>-</sup>, and half a molecule of bimb with triclinic system space group *P*-1. As shown in figure 2(a), each Mn<sup>II</sup> is six-coordinate by five carboxylate oxygens [Mn–O, ranging from 2.1241(13) to 2.3428(13) Å] and one nitrogen from bimb [Mn(1)–N(1) = 2.2199(15) Å], showing a

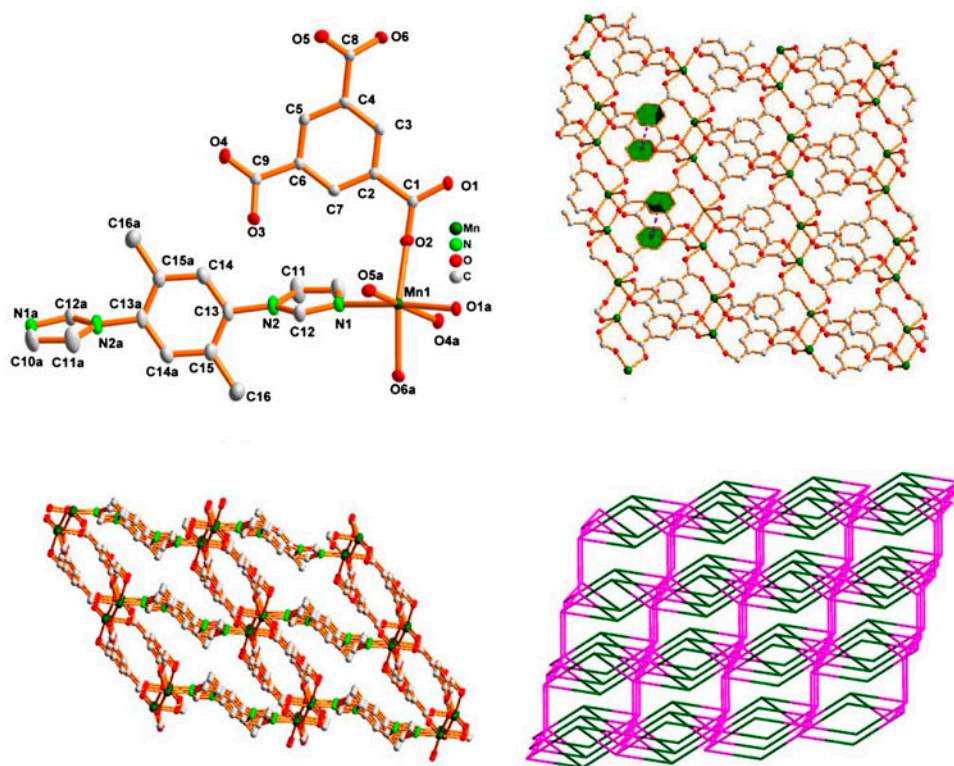


Figure 2. (a) Coordination environment around Mn(II) with 50% thermal ellipsoids drawn at 50% probability. All hydrogens were omitted for clarity; (b) the 2-D layer structure formed by Mn(II) and carboxylate ligands; (c) the 3-D structure for **2**; (d) the (3,6)-connected topology for **2**. The pink lines: bimb ligands. The other color lines: carboxylate ligands (see <http://dx.doi.org/10.1080/00958972.2015.1018194> for color version).

distorted octahedral geometry. The partially deprotonated  $\text{Hbtc}^{2-}$  coordinated to five Mn(II) ions and three carboxylate groups adopt  $\mu_1: \eta^0/\eta^1$  (monodentate) and  $\mu_2: \eta^1/\eta^1$  (*bis*-monodentate) coordination modes, including a protonated coordination mode. The existence of  $-\text{COOH}$  in  $\text{Hbtc}^-$  (partial deprotonation of  $\text{H}_3\text{btc}$ ) was confirmed by IR spectral data, since a band of  $1682\text{ cm}^{-1}$  was observed in the IR spectrum of **2**. The carboxylate groups containing O1, O2, O5, and O6 are  $\mu_2: \eta^1/\eta^1$  coordination in which the Mn–O distances are 2.1243(13) Å, 2.1449(13) Å, 2.1241(13) Å, and 2.2754(12) Å. The carboxylate groups containing O3 and O4 are  $\mu_1: \eta^0/\eta^1$  coordination in which Mn–O distance is 2.3428(13) Å. The carboxylates connect Mn(II) to construct a 2-D layer structure [figure 2(b)], in which the adjacent Mn–Mn distance is 4.472 Å. In the 2-D layer, there exist  $\pi$ – $\pi$  stacking interactions with the centroid to centroid distance of 3.507 Å between the phenyl rings ( $\text{Cg}(2)$  is defined by C2, C3, C4, C5, C6, and C7). The bimb ligands as pillars coordinate to Mn(II) ions which construct a 3-D framework and also result in the Mn(II) ions as 6-connected nodes [figure 2(c)]. Thus, the 3-D framework can be regarded as (3,6)-connected topological net with point symbol  $(3.4.5).(3^2.4^2.5.6^8.7^2)$  [figure 2(d)].

Some related Mn(II) CPs are cited as structural comparisons. Guo and coworkers reported a series of Mn(II) CPs,  $[\text{Mn}(\text{Hdpa})_2(4,4'\text{-bipy})_2]_n$ ,  $[\text{Mn}(\text{dpa})(1,10\text{-phen})(\text{H}_2\text{O})]_n$ ,

and  $[\text{Mn}(\text{dpa})(2,2'\text{-bipy})]_n$  ( $\text{H}_2\text{dpa}$  = 2,4'-biphenyl-dicarboxylic acid, 4,4'-bipy = 4,4'-bipyridine, 1,10-phen = 1,10-phenanthroline, and 2,2'-bipy = 2,2'-bipyridine). In  $[\text{Mn}(\text{Hdpa})_2(4,4'\text{-bipy})_2]_n$ ,  $[\text{Mn}(\text{dpa})(1,10\text{-phen})(\text{H}_2\text{O})]_n$ , and  $[\text{Mn}(\text{dpa})(2,2'\text{-bipy})]_n$ , the Mn–O bond distances range from 2.147 Å to 2.319 Å, similar to **1** and **2**. In **1**, the Mn–O bond lengths with  $\mu_2: \eta^1/\eta^1$  coordination mode are 2.0492(14)–2.1820(15) Å, which are similar to the Mn–O bond distances with  $\mu_2: \eta^1/\eta^1$  coordination of  $[\text{Mn}(\text{Hdpa})_2(4,4'\text{-bipy})_2]_n$  and  $[\text{Mn}(\text{dpa})(2,2'\text{-bipy})]_n$  [39]. Yang and coworkers reported  $\{[\text{Mn}_3(\text{bpt})_2(\text{bib})_2(\text{H}_2\text{O})_2] \cdot (\text{H}_2\text{O})_2\}_n$  [ $\text{H}_3\text{bpt}$  = biphenyl-3,4',5-tricarboxylic acid and bib = 1,4-bis(imidazolyl)benzene], in which the Mn–O distances range from 2.092(2) to 2.415(2) Å. The carboxylates are  $\mu_2: \eta^1/\eta^1$ ,  $\mu_2: \eta^1/\eta^2$  and  $\mu_1: \eta^1/\eta^1$ . The Mn–O distances of  $\mu_2: \eta^1/\eta^2$  are similar to the Mn–O distance in **1** [40]. Zhang and coworkers reported  $[\text{Mn}(\text{tda})(\text{ip})(\text{H}_2\text{O})]_n$  [ $\text{H}_2\text{tda}$  = thiophene-2,5-dicarboxylic acid, ip = 1H-imidazo[4,5-f][1, 10]-phenanthroline]. The Mn–O distances are 2.1189(11) to 2.2386(16) Å and the carboxylates are  $\mu_2: \eta^1/\eta^2/\mu_1: \eta^1/\eta^0$ , all of which are similar to **2** [41]. Sun and coworkers reported  $[\text{Mn}(\text{L})]$  and  $[\text{Mn}(\text{L})(\text{pybim})]$  [ $\text{H}_2\text{L}$  = 5-(benzimidazol-1-ylmethyl)isophthalic acid and pybim = 2-(pyridin-2-yl)-1H-benzimidazole]. The Mn–O distances range from 2.0699(15) to 2.468(2) and the carboxylate groups are  $\mu_1: \eta^1/\eta^1$ ,  $\mu_2: \eta^1/\eta^1$  and  $\mu_1: \eta^1/\eta^0$ , similar to the Mn–O distances of **1** and **2** and coordination modes for carboxylates [42]. In **1** and **2**, the adjacent Mn...Mn distances are 3.586 Å, 4.472 Å, and 5.003 Å, respectively, similar to  $[\text{Mn}(\text{dpa})(1,10\text{-phen})(\text{H}_2\text{O})]_n$  [Mn...Mn, 3.471 Å],  $[\text{Mn}(\text{dpa})(2,2'\text{-bipy})]_n$  [Mn...Mn, 3.462 Å],  $[\text{Mn}(\text{L})]$  [Mn...Mn, 3.96 Å], and  $[\text{Mn}(\text{aip})(\text{phen})]_n$  ( $\text{H}_2\text{aip}$  = 5-aminoisophthalic acid, phen = 1,10-phenanthroline) [Mn...Mn, 4.4465 Å] [43].

### 3.2. Thermogravimetric analyses and XRPD analyses

The TG curve of **1** shows that **1** is stable to 370 °C and then a weight loss to 800 °C may be attributed to loss of organic ligands (obs. 78.96%, calcd 79.12%) [figure S1(a), see online supplemental material at <http://dx.doi.org/10.1080/00958972.2015.1018194>]. The TG curve for **2** exhibits an initial weight loss starting at 210 °C with the observed weight loss of 81.58% (calcd 81.44%) [figure S1(b)]. The resulting residue for **1** and **2** is MnO.

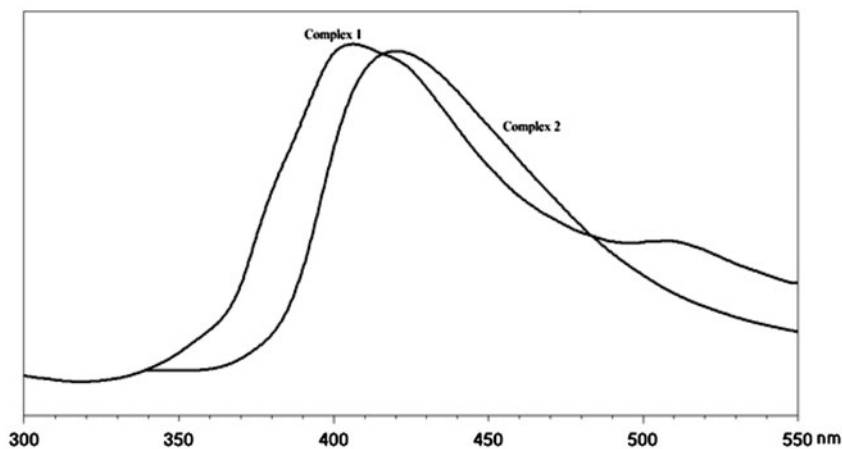


Figure 3. The luminescent emission spectra for **1** and **2** in the solid state at room temperature.



To confirm the purity of the samples, **1** and **2** are measured by XRPD. Experimental and simulated XRPD patterns for **1** and **2** are shown in figure S2. All peaks in the measured curves approximately match the simulated curves generated from single-crystal diffraction data, which confirms the phase purity of the as-synthesized products.

### 3.3. Luminescent properties

In the solid state, **1** and **2** show photoluminescence at room temperature (figure 3), exhibiting emission at *ca.* 406 nm ( $\lambda_{\text{ex}} = 315$  nm) and 422 nm ( $\lambda_{\text{ex}} = 336$  nm), respectively. The bimb ligands show emission at 421 nm [44]. The emissions of **1** and **2** are different from the free ligands, which might be assigned to intraligand emission excited state [45, 46].

## 4. Conclusion

We obtained two new Mn(II) CPs based on carboxylate and imidazole-containing ligands. Complex **1** is an unusual binodal (3,7)-connected 3-D architecture with point symbol  $(4^4.6^{17}).(6^3)$ . Complex **2** is a rare (3,6)-connected 3-D structure with point symbol  $(3.4.5).(3^2.4^2.5.6^3.7^2)$ . Complexes **1** and **2** show emissions in the solid state at room temperature.

## Supplementary material

Crystallographic data for the structural analysis have been deposited with the Cambridge Crystallographic Data Center, CCDC reference numbers 992883 (for **1**) and 992884 (for **2**). These data can be obtained free of charge at <http://www.ccdc.cam.ac.uk> (or Cambridge Crystallographic Data Center, 12 Union Road, Cambridge CB2 1EZ, UK; Fax: +44-1223-336-033; E-mail: [deposit@ccdc.cam.ac.uk](mailto:deposit@ccdc.cam.ac.uk)).

## Funding

We thank the financial support from the Natural Science Foundation of China [grant number 21401075], Shandong Provincial Natural Science Foundation [grant number ZR2012BL01], A Project of Shandong Province Higher Educational Science and Technology Program [grant number J12LD54].

## References

- [1] M. O'Keeffe, O.M. Yaghi. *Chem. Rev.*, **112**, 675 (2012).
- [2] I.A.V. Baburin, A. Blatov, L. Carlucci, G. Ciani, D.M. Proserpio. *J. Solid State Chem.*, **178**, 2471 (2005).
- [3] Q.X. Yang, X.Q. Chen, Z.J. Chen, Y. Hao, Y.Z. Li, Q.Y. Lu, H.G. Zheng. *Chem. Commun.*, **48**, 10016 (2012).
- [4] G.L. Wen, Y.Y. Wang, Y.N. Zhang, G.P. Yang, A.Y. Fu, Q.Z. Shi. *CrystEngComm*, **11**, 1519 (2009).
- [5] J. Li, J. Tao, R.B. Huang, L.S. Zheng. *Inorg. Chem.*, **51**, 5988 (2012).
- [6] S.Y. Qian, H. Zhou, A.H. Yuan, Y. Song. *Cryst. Growth Des.*, **11**, 5676 (2011).
- [7] X.D. Zheng, Y.L. Hua, R.G. Xiong, J.Z. Ge, T.B. Lu. *Cryst. Growth Des.*, **11**, 302 (2011).
- [8] S. Barman, H. Furukawa, O. Blacque, K. Venkatesan, O.M. Yaghi, H. Berke. *Chem. Commun.*, **46**, 7981 (2010).
- [9] C.T. He, J.Y. Tian, S.Y. Liu, G.F. Ouyang, J.P. Zhang, X.M. Chen. *Chem. Sci.*, **4**, 351 (2012).

- [10] L.Q. Han, Y. Yan, F.X. Sun, K. Cai, T. Borjigin, X.J. Zhao, F.Y. Qu, G.S. Zhu. *Cryst. Growth Des.*, **13**, 1458 (2013).
- [11] Y. Liu, J.R. Li, W.M. Verdegaal, T.F. Liu, H.C. Zhou. *Chem. Eur. J.*, **19**, 5637 (2013).
- [12] G. Akiyama, R. Matsuda, H. Sato, A. Hori, M. Takata, S. Kitagawa. *Microporous Mesoporous Mater.*, **157**, 89 (2012).
- [13] M.B. Lalonde, O.K. Farha, K.A. Scheidt, J.T. Hupp. *ACS Catal.*, **2**, 1550 (2012).
- [14] K.S. Jeong, Y.B. Go, S.M. Shin, S.J. Lee, J. Kim, O.M. Yaghi, N. Jeong. *Chem. Sci.*, **2**, 877 (2011).
- [15] H. Yang, F. Wang, Y.X. Tan, Y. Kang, T.-H. Li. *Chem. Asian J.*, **7**, 1069 (2012).
- [16] M.J. Sie, Y.J. Chang, P.W. Cheng, P.T. Kuo, C.W. Yeh, C.F. Cheng, J.D. Chen, J.C. Wang. *CrystEngComm*, **14**, 5505 (2012).
- [17] X.J. Li, F.L. Jiang, M.Y. Wu, S.Q. Zhang, Y.F. Zhou, M.C. Hong. *Inorg. Chem.*, **51**, 4116 (2012).
- [18] F. Guo, F. Wang, H. Yang, X.L. Zhang, J. Zhang. *Inorg. Chem.*, **51**, 9677 (2012).
- [19] T. Kundu, S.C. Sahoo, R. Banerjee. *Chem. Commun.*, **48**, 4998 (2012).
- [20] L. Qin, J.S. Hu, Y.Z. Li, H.G. Zheng. *Cryst. Growth Des.*, **12**, 403 (2012).
- [21] K.K. Bisht, E. Suresh. *Cryst. Growth Des.*, **13**, 664 (2013).
- [22] J. Yao, Z.D. Lu, Y.Z. Li, J.G. Lin, X.Y. Duan, S. Gao, Q.J. Meng, C.S. Lu. *CrystEngComm*, **10**, 1379 (2008).
- [23] L.F. Ma, M.L. Han, J.H. Qin, L.Y. Wang, M. Du. *Inorg. Chem.*, **51**, 9431 (2012).
- [24] K. Jiang, L.F. Ma, X.Y. Sun, L.Y. Wang. *CrystEngComm*, **13**, 330 (2010).
- [25] F. Guo, B.Y. Zhu, M.L. Liu, X.L. Zhang, J. Zhang, J.P. Zhao. *CrystEngComm*, **15**, 6191 (2013).
- [26] F. Guo, B.Y. Zhu, G.L. Xu, M.M. Zhang, X.L. Zhang, J. Zhang. *J. Solid State Chem.*, **199**, 42 (2013).
- [27] H.L. Jia, Y.X. Li. *Z. Anorg. Allg. Chem.*, **640**, 1490 (2014).
- [28] L.P. Xu, X.M. Wang. *Z. Anorg. Allg. Chem.*, **640**, 1680 (2014).
- [29] M.M. Zhang, F. Guo. *Synth. React. Inorg. Met-Org. Chem.*, **44**, 541 (2014).
- [30] N.N. Ma, F. Guo. *J. Inorg. Organomet. Polym.*, **23**, 1177 (2013).
- [31] G.L. Xu, F. Guo. *Inorg. Chem. Commun.*, **27**, 146 (2013).
- [32] S. Barman, H. Furukawa, O. Blacque, K. Venkatesan, O.M. Yaghi, G.X. Jin, H. Berke. *Chem. Commun.*, **47**, 11882 (2011).
- [33] M.L. Foo, S. Horike, S. Kitagawa. *Inorg. Chem.*, **50**, 11853 (2011).
- [34] G.M. Sheldrick, *SAINTE Software Reference Manual*, Bruker AXS, Madison, WI (1998).
- [35] G.M. Sheldrick, *SHELXTL NT, (Version 5.1), Program for Solution and Refinement of Crystal Structures*, University of Göttingen, Göttingen, Germany (1997).
- [36] V.A. Blatov. *IUCr CompComm Newsletter*, **7**, 4 (2006).
- [37] V.A. Blatov, A.P. Shevchenko, V.N. Serezhkin. *J. Appl. Crystallogr.*, **33**, 1193 (2000).
- [38] V.A. Blatov, M. O'Keefe, D.M. Proserpio. *CrystEngComm*, **12**, 44 (2009), Available online at: <http://www.topos.ssu.Samara.ru>.
- [39] F. Guo, B.Y. Zhu, Y.L. Song, X.L. Zhang. *J. Coord. Chem.*, **63**, 1304 (2010).
- [40] Y.L. Lu, W.J. Zhao, X. Feng, Y. Chai, Z. Wu, X.W. Yang. *J. Coord. Chem.*, **66**, 473 (2013).
- [41] X.L. Zhang, K. Cheng. *J. Coord. Chem.*, **65**, 3019 (2012).
- [42] H.W. Kuai, T. Okamura, W.Y. Sun. *J. Coord. Chem.*, **66**, 473 (2012).
- [43] J.J. Wang, Q.L. Bao, J.X. Chen. *J. Coord. Chem.*, **66**, 2578 (2013).
- [44] G.L. Xu, F. Guo. *Inorg. Chem. Commun.*, **27**, 146 (2013).
- [45] V.W.W. Yam, K.K.W. Lo. *Chem. Soc. Rev.*, **28**, 323 (1999).
- [46] S.J. Wang, S.S. Xiong, L.X. Song, Z.Y. Wang. *CrystEngComm*, **11**, 896 (2009).